



## CO<sub>2</sub> Capture-Induced Electrolytes Using Tertiary Diamines

Eri Yoshida\*

Department of Applied Chemistry and Life Science, Toyohashi University of Technology,  
Toyohashi, Japan

\*Corresponding author: [yoshida.eri.gu@tut.jp](mailto:yoshida.eri.gu@tut.jp)

### Abstract

With the aim of early reducing global warming, CO<sub>2</sub> capture-induced electrolytes were created using tertiary diamines of *N,N,N',N'*-tetramethylethylenediamine (TM-Et), *N,N,N',N'*-tetramethyl-1,3-propanediamine (TM-Pr), *N,N,N',N'*-tetramethyl-1,6-hexanediamine (TM-Hex), bis(2-dimethylaminoethyl) ether (BDM-Ee), *N,N'*-dimethylpiperazine (DM-Pip), 1,4-diazabicyclo[2.2.2]octane (DABCO), and hexamethylenetetramine (HMT). A <sup>13</sup>C NMR analysis, coupled with viscosity measurements revealed that the electrolytes were obtained by the diamines capturing carbonic acid generated by CO<sub>2</sub> dissolving in water and produced through the formation of the diammonium carbonate, followed by the transformation into the bicarbonate. The electroconductivity (EC) of the electrolytes was independent of the counter anions and dependent only on the protonated diamine concentration. The electrolytes were more effectively formed at high temperature, despite a decrease in the CO<sub>2</sub> solubility in water. The basicity and structure of the diamines also affected the EC. TM-Et, DM-Pip, and DABCO that show a low basicity and have two methylenes between the N atoms, produced only half of the EC for the highly basic TM-Pr, TM-Hex, and BDM-Ee based on formation of an intramolecular five-membered ring involving a proton through hydrogen bonding. On the

other hand, HMT produced no EC due to its very low basicity. The electrolyte of the diammonium bicarbonate was transformed into the carbonate by introducing Ar. However, this transformation was reversed by introducing CO<sub>2</sub> again, suggesting the repeatable use of the electrolytes.

**Keywords:** *CO<sub>2</sub> capture, tertiary diamines, electrolytes, carbonic acid, electroconductivity, bicarbonate, carbonate*

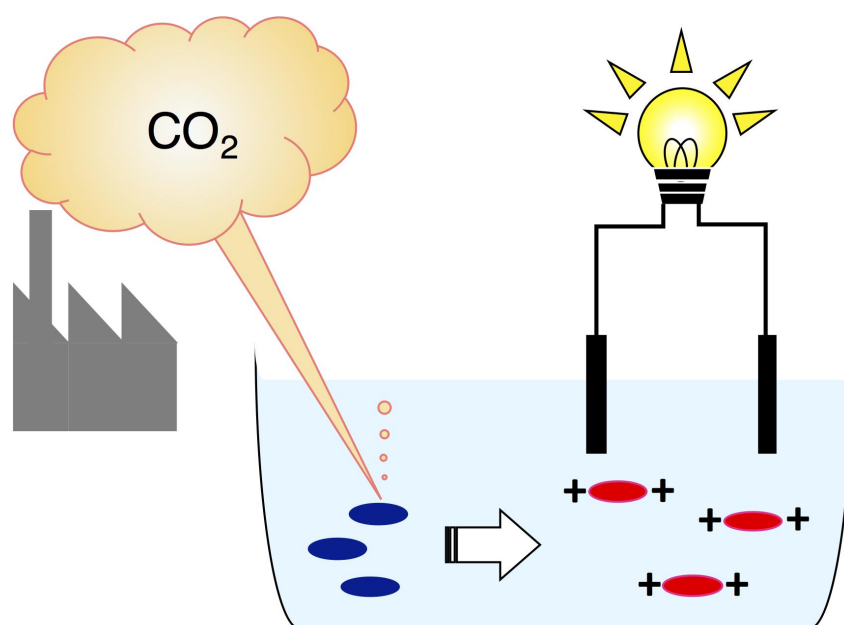
## 1. Introduction

Global warming has been a pressing issue worldwide. The warming by greenhouse gases, mainly CO<sub>2</sub>, has been intensified year by year and caused many severe disasters and environmental problems; the extreme weather [1], large-scale forest fires [2], coral bleaching [3, 4], marine ecosystem changes [5], and a drop in the global economic productivity [6]. With the aim of reducing the greenhouse gas emissions, CO<sub>2</sub> capture and utilization technologies have been developed. Examples include the ocean sequestration [7], separation and recovery using membranes [8], fixation by alga [9, 10] and bacteria [11, 12], and also fixation through addition reactions to organic reagents, such as alcohols, amines [13], olefins, and heterocyclic compounds [14-18]. The use of CO<sub>2</sub> as a solvent under supercritical conditions in the food and textile industries [19-22] and the recent use as an external stimulus for responsive molecular aggregates [23-25] provided the greenhouse gas with beneficial applications. The substrates for chemically capturing CO<sub>2</sub> are mainly classified into four groups; amines [26, 27], metals and metal oxides [28], ionic liquids [29], and porous materials of zeolites [30], silica [31], and nanotubes [32]. Methods featuring combinations of these substrates have also been developed.

Amines effectively capture CO<sub>2</sub> in solution and also on the surface of materials based on their easy modifications [27]. While primary and secondary amines react with CO<sub>2</sub> to form carbamate, tertiary amines capture CO<sub>2</sub> in the form of a carbonate and bicarbonate in an aqueous solution [33]. In particular, tertiary diamines effectively serve as the sorbent [34]. It has been reported that ammonium bicarbonate and its carbonate have environmentally important roles in the respective technologies and industries. Ammonium bicarbonate serves as a removing agent for SO<sub>2</sub> and NO<sub>x</sub>, the major source of air pollution [35], while ammonium carbonate efficiently recovers pure uranium from the transuranic elements and

fission products by dissolving uranium oxide as its carbonate in water during the reprocessing of spent nuclear fuels [36].

In order to improve the reduction in the CO<sub>2</sub> emissions, it is crucial not only to effectively capture CO<sub>2</sub>, but also to utilize the products obtained by capturing CO<sub>2</sub>. There are few papers that have focused on the products by CO<sub>2</sub> capture. Recently, Hatton and coworker released a publication concerning the electrodes that generated a current by CO<sub>2</sub> capture based on the reductive addition of CO<sub>2</sub> to quinones [37]. It was found that tertiary diamines produced electrolytes by capturing CO<sub>2</sub> in water. This paper describes the formation of CO<sub>2</sub> capture-induced electrolytes using tertiary diamines and their electrical properties (Scheme 1).



**Scheme 1.** A schematic image of the CO<sub>2</sub> capture-induced electrolytes.

## 2. Experimental

### 2.1. Instrumentation

Electroconductivity (EC) and pH were measured using a Hanna Instruments HI99300N portable EC/TDS/°C meter and HI991002N portable pH/ORP/°C meter, respectively. NMR measurements were conducted using a Jeol ECS500 FT NMR spectrometer. The viscosity was measured at 25°C using an A&D SV-10 vibro viscometer equipped with an Eyela digital Uni Ace UA-100 temperature circulator.

### 2.2. Materials

All amines and acids were purchased from Tokyo Chemical Industry Co. Ltd. *N,N,N',N'*-Tetramethylethylenediamine (TM-Et) was purified by distillation over sodium. *N,N,N',N'*-Tetramethyl-1,3-propanediamine (TM-Pr), *N,N,N',N'*-tetramethyl-1,6-hexanediamine (TM-Hex), and *N,N'*-dimethylpiperazine (DM-Pip) were distilled over calcium hydride under reduced pressure. Bis(2-dimethylaminoethyl) ether (BDM-Ee) was distilled over sodium under reduced pressure. 1,4-Diazabicyclo[2.2.2]octane (DABCO) and hexamethylenetetramine (HMT) were used as received. Acetic acid and glutaric acid were also used without further purification. Ultrapure water was obtained using a Merck Milli-Q® Integral MT-5 water purification system. CO<sub>2</sub> with over 99.995 vol% purity and Ar with over 99.999 vol% purity were purchased from Taiyo Nippon Sanso Corporation.

### **2.3. CO<sub>2</sub> capture-induced electrolytes: General procedure**

TM-Hex (3.000 g, 17.41 mmol) was dissolved in ultrapure water (20 mL). CO<sub>2</sub> was bubbled to this diamine solution at the flow speed of 250 mL/min using a flow meter. The solution was subjected to pH and viscosity measurements at the designated times. Part of the solution (1 mL) was taken using a syringe and mixed with ultrapure water (14 mL) to subject to an EC measurement due to the upper limitation of the EC meter.

### **2.4. Alternate CO<sub>2</sub>-Ar introduction to a TM-Hex solution**

TM-Hex (4.527 g, 26.27 mmol) was dissolved in ultrapure water (20 mL). CO<sub>2</sub> was introduced by bubbling to this diamine solution at the flow speed of 250 mL/min for 2 h at room temperature. Ar instead of CO<sub>2</sub> was introduced to the solution at 500 mL/min for 4 h. CO<sub>2</sub> instead of Ar was introduced again to the solution at 250 mL/min for 1 h. The solution during the respective stages was subjected to pH and EC measurements at the designated times.

## **3. Results and discussion**

For the purpose of obtaining CO<sub>2</sub> capture-induced electrolytes using tertiary diamines in water, an aqueous solution of the diamine was evaluated based on changes in the pH and EC. As CO<sub>2</sub> was introduced into an aqueous TM-Hex solution by bubbling, the pH showed a two-step decrease; the first rapid decrease in a few minutes, followed by the second gradual decrease up to 60 min (Figure 1a). This two-step change in pH suggests that the diammonium

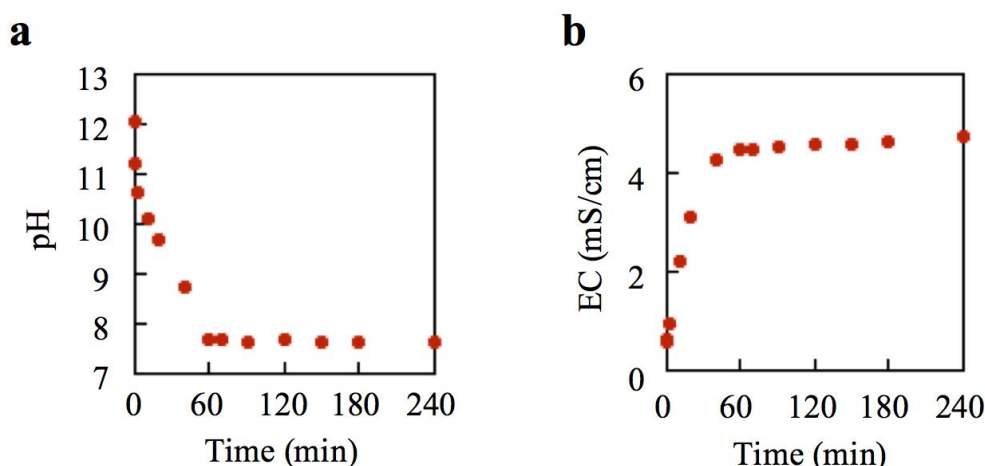
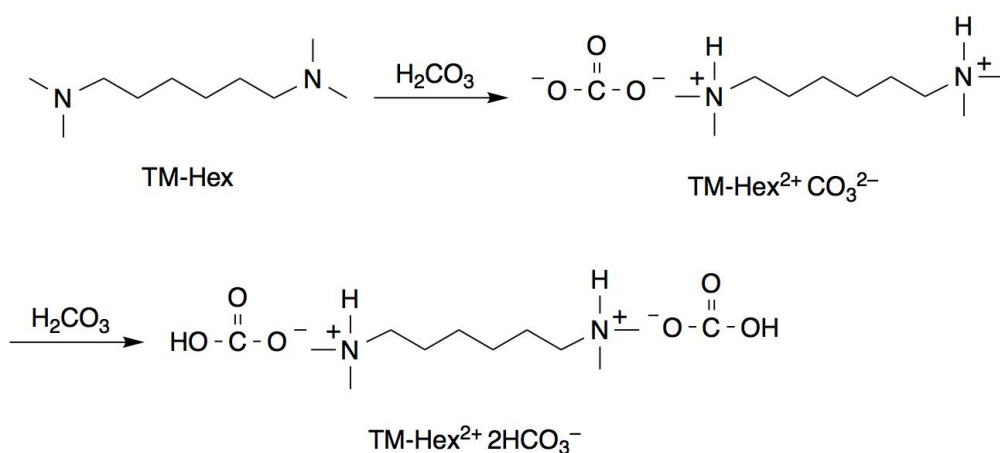


**Figure 1.** The variations in the pH (a) and EC (b) of a TM-Hex solution by introducing CO<sub>2</sub>. CO<sub>2</sub> flow speed = 250 mL/min for the solution (20 mL). [TM-Hex]<sub>0</sub> = 0.871 M.



**Scheme 2.** Formation of the diammonium carbonate by TM-Hex capturing carbonic acid, followed by transformation into the bicarbonate.

carbonate (TM-Hex<sup>2+</sup>CO<sub>3</sub><sup>2-</sup>) was formed during the first stage, and the carbonate transformed into the bicarbonate (TM-Hex<sup>2+</sup>2HCO<sub>3</sub><sup>-</sup>) during the second stage (Scheme 2). The bicarbonate solution became steady at pH = 7.5 over 60 min and did not decrease its pH by a further CO<sub>2</sub> introduction. It was found that the bicarbonate solution did not dissolve CO<sub>2</sub> any more due to the limited solubility of CO<sub>2</sub>. The limited CO<sub>2</sub> solubility in the bicarbonate solution was supported by the fact that pure water became steady at pH = 3.9 by the CO<sub>2</sub> introduction (Figure 2). The CO<sub>2</sub> introduction also provided the solution with an electrical property. By introducing CO<sub>2</sub>, the EC of the solution consecutively increased and reached a steady state (Figure 1b). Pure water produced no EC by the CO<sub>2</sub> introduction, indicating that

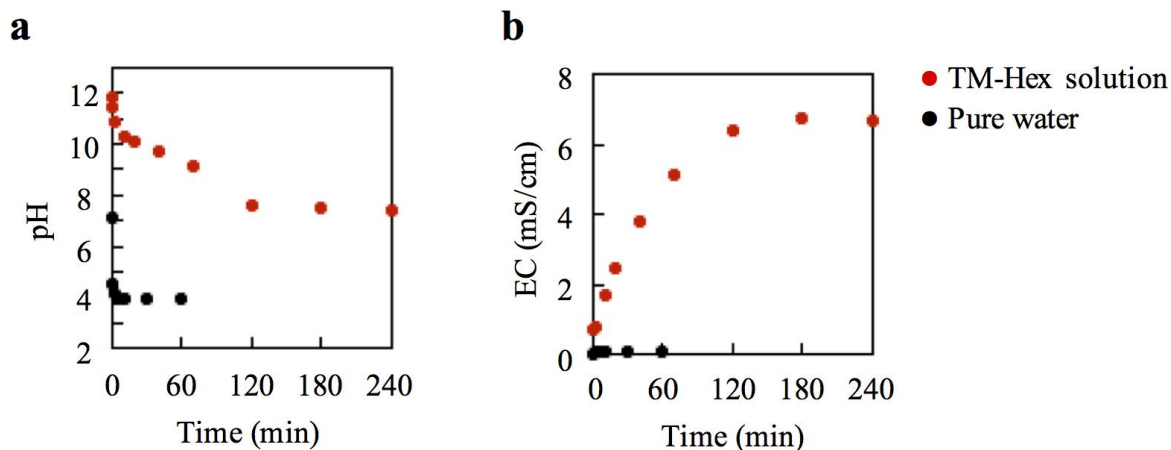


**Figure 2.** The variations in the pH (a) and EC (b) of a TM-Hex solution and pure water by introducing CO<sub>2</sub>. CO<sub>2</sub> flow speed = 500 mL/min for the solution (200 mL) or water. [TM-Hex]<sub>0</sub> = 0.871 M.

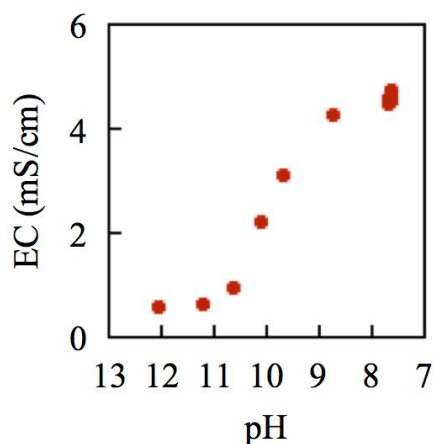


**Figure 3.** The variation in the EC vs. pH for a TM-Hex solution by CO<sub>2</sub> introduction. CO<sub>2</sub> flow speed = 250 mL/min for the solution (20 mL). [TM-Hex]<sub>0</sub> = 0.871 M.

the EC was caused by the diamine capturing CO<sub>2</sub>. As can be seen in Figure 3, the EC increased with a decrease in pH, implying that the EC was generated by the capture of carbonic acid. No phase change in the EC, unlike the pH change, indicated that the EC was independent of the counter anions and dependent only on the protonated diamine concentration. This cation-dependence of EC is understandable based on ECs of NaCl and NH<sub>4</sub><sup>+</sup>HCO<sub>3</sub><sup>-</sup>; the EC of the TM-Hex<sup>2+</sup>2HCO<sub>3</sub><sup>-</sup> solution (EC = 6.72 mS/cm) was about half that of the solutions of NaCl (EC = 11.92 mS/cm) and NH<sub>4</sub><sup>+</sup>HCO<sub>3</sub><sup>-</sup> (EC = 10.43 mS/cm) for the same ion equivalent.

The viscosity measurement of the TM-Hex solution during the CO<sub>2</sub> introduction elucidated

the transformation of the carbonate into the bicarbonate. Figure 4 shows the variation in

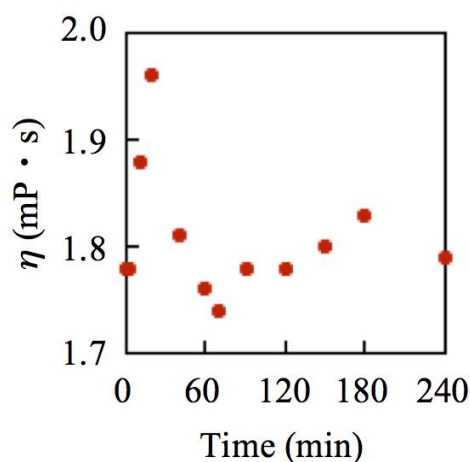
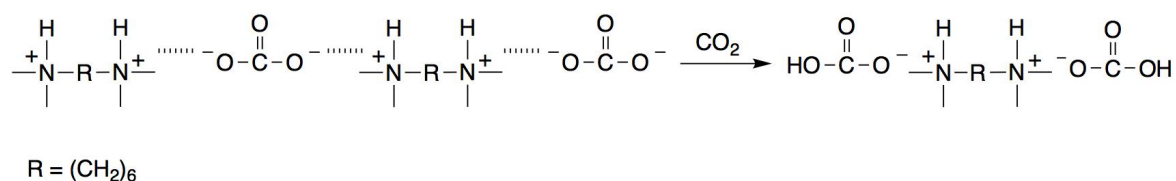


**Figure 4. The variation in viscosity of a TM-Hex solution during CO<sub>2</sub> introduction.**  
**CO<sub>2</sub> flow speed = 250 mL/min for the solution (20 mL). [TM-Hex]<sub>0</sub> = 0.871 M.**

viscosity of the solution during the CO<sub>2</sub> introduction. The viscosity was immediately increased by the CO<sub>2</sub> introduction and continued to increase for a few minutes. The viscosity rapidly decreased up to 60 min, then it gradually increased and decreased by further CO<sub>2</sub> introduction. The first immediate increase in viscosity was based on the alternating bonding of the protonated TM-Hex and carbonate through the electrostatic interaction, and the following decrease was due to the disruption of this alternating bonding by the transformation of the carbonate into the bicarbonate (Scheme 3). The reactions of the diamine with GA and AA instead of CO<sub>2</sub> supported the first sudden increase in viscosity based on the alternating electrostatic bonding formation and the second gradual increase due to the carbonate-to-bicarbonate transformation (Figure 5). The viscosity change by GA was about twice that by AA for the equal molar equivalence of COOH based on the alternating electrostatic bonding between the protonated TM-Hex and glutarate. AA also caused a slight increase in the viscosity due to the electrolyte formation. The plots of viscosity of the diamine solution vs. pH for GA and AA, coupled with the CO<sub>2</sub> introduction are shown in Figure 6. The comparison of the viscosity change revealed that the bicarbonate electrolyte caused no



**Scheme 3. The alternating bonding of the protonated TM-Hex and carbonate through the electrostatic interaction and the transformation into the bicarbonate.**

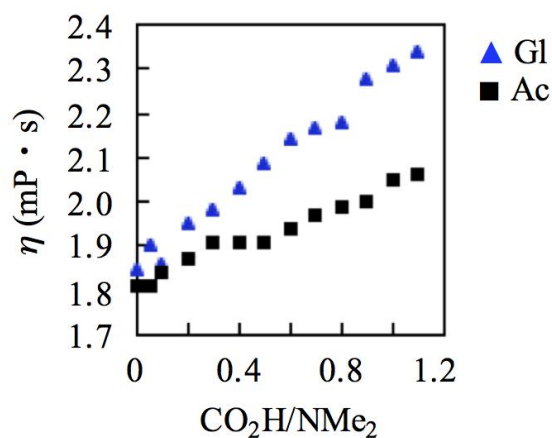


**Figure 5. The variation in viscosity of a TM-Hex solution by adding Gl (▲) and Ac (■).**

[TM-Hex]<sub>0</sub> = 0.871 M.

increase in viscosity. The bicarbonate anions have a negligible interaction with each other due to their non-dissociated form. In addition, there was no difference in EC of the diamine

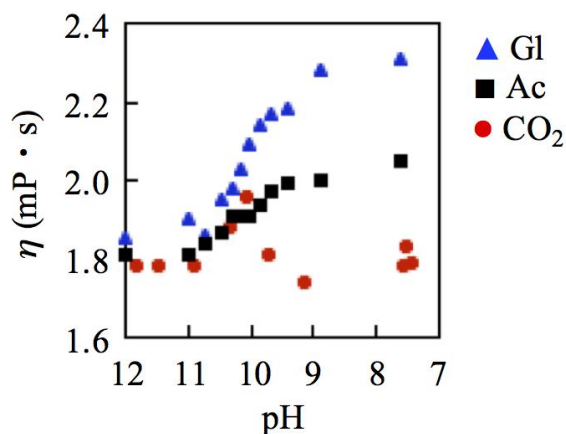


**Figure 6. The variation in viscosity of a TM-Hex solution vs. pH for Gl (▲), Ac (■), and CO<sub>2</sub> introduction (●). [TM-Hex]<sub>0</sub> = 0.871 M. CO<sub>2</sub> flow speed = 250 mL/min for the solution (20 mL).**

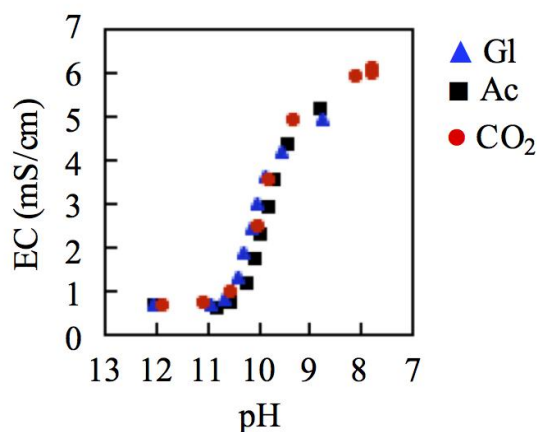


Figure 7. The variation in the EC of a TM-Hex solution vs. pH for Gl ( $\blacktriangle$ ), Ac ( $\blacksquare$ ), and CO<sub>2</sub> introduction ( $\bullet$ ). [TM-Hex]<sub>0</sub> = 1.314 M. CO<sub>2</sub> flow speed = 250 mL/min for the solution (20 mL).

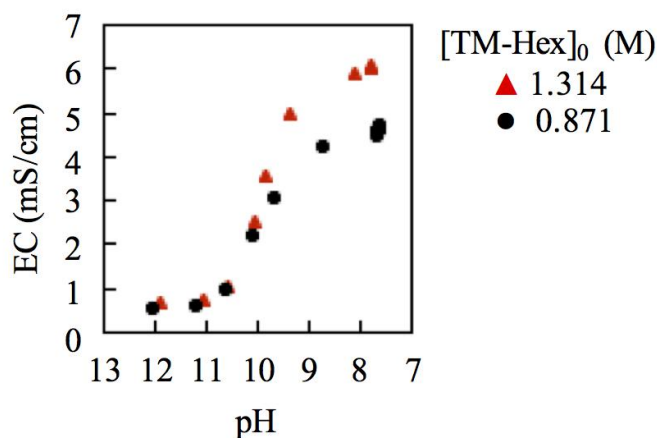
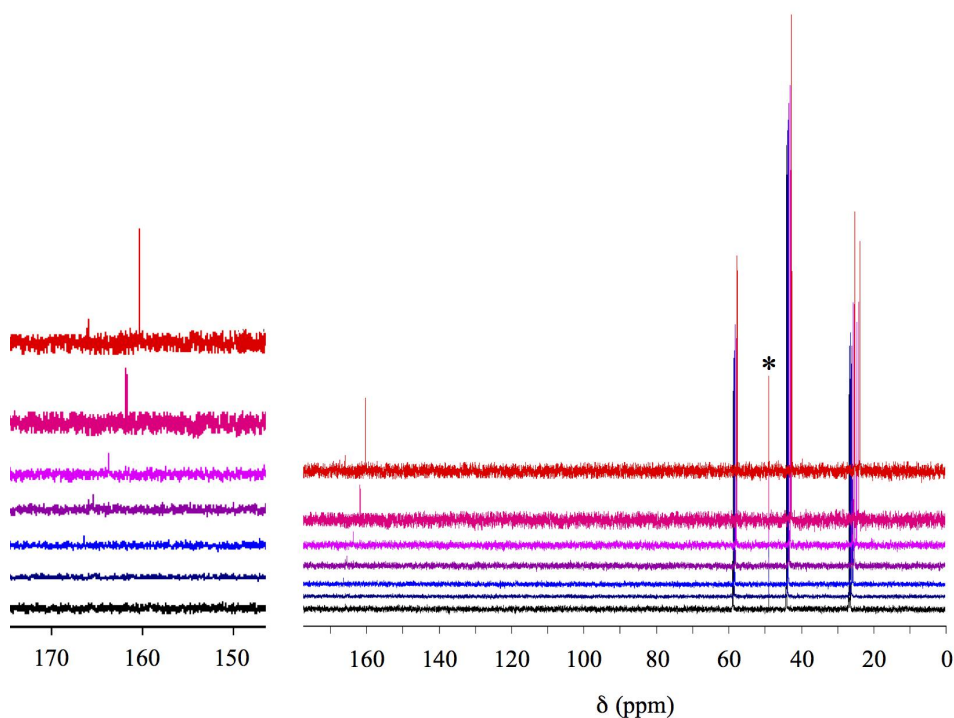


Figure 8. The variation in the EC of a TM-Hex solution vs. pH for different concentrations: 1.314 M ( $\blacktriangle$ ) and 0.871 M ( $\bullet$ ). CO<sub>2</sub> flow speed = 250 mL/min for the solution (20 mL).

solution among GA, AA, and the CO<sub>2</sub> introduction supporting the fact that the EC was dependent only on the protonated diamine concentration (Figures 7 and 8).

A <sup>13</sup>C NMR analysis confirmed the carbonate-to-bicarbonate transformation. Figure 9 shows <sup>13</sup>C NMR spectra of the solution at each CO<sub>2</sub> introduction time. The signal of the carbonyl carbon was discerned from 10 minutes after the introduction of CO<sub>2</sub> to the end of the reaction.



**Figure 9.**  $^{13}\text{C}$  NMR spectra of a TM-Hex solution during  $\text{CO}_2$  introduction for 0, 1.5, 10, 20, 40, 70, and 120 min (from the bottom). \* Methanol standard. Solvent:  $\text{D}_2\text{O}$ .  $\text{CO}_2$  flow speed = 500 mL/min for the solution (200 mL).  $[\text{TM-Hex}]_0 = 0.871 \text{ M}$ .

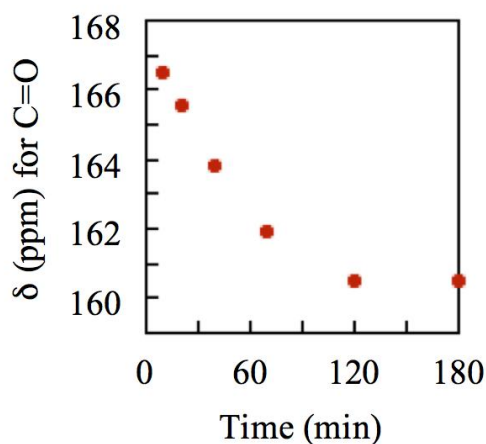


**Figure 10.** The variation in the chemical shift of the carbonyl carbon during  $\text{CO}_2$  introduction.

The signal was shifted to the higher side of a magnetic field with time, accompanied by an increase in the signal intensity. The variation in the chemical shift of the signal with time is shown in Figure 10. A signal for the carbonyl carbon of the ammonium bicarbonate,  $\text{NH}_4^+\text{HCO}_3^-$ , was observed at 160.53 ppm in  $\text{D}_2\text{O}$ , while that of ammonium carbonate ( $2\text{NH}_4^+\text{CO}_3^{2-}$ ) was at 165.82 ppm in the presence of aqueous ammonia. Based on these

chemical shifts of the carbonyl carbons, it was proved that the TM-Hex<sup>2+</sup>carbonate was transformed into the bicarbonate by continuous CO<sub>2</sub> introduction. Furthermore, the <sup>1</sup>H NMR analysis revealed that a proton captured by TM-Hex freely moved in the solution without being restricted to a single amino group. As shown in Figure 11, signals originating from TM-Hex were successively shifted to the lower side of the magnetic field by the CO<sub>2</sub> introduction between the signals for TM-Hex non-protonated and protonated by capturing carbonic acid. This successive shift in the signals indicated all the amino groups were engaged in the interaction with the carbonic acid.

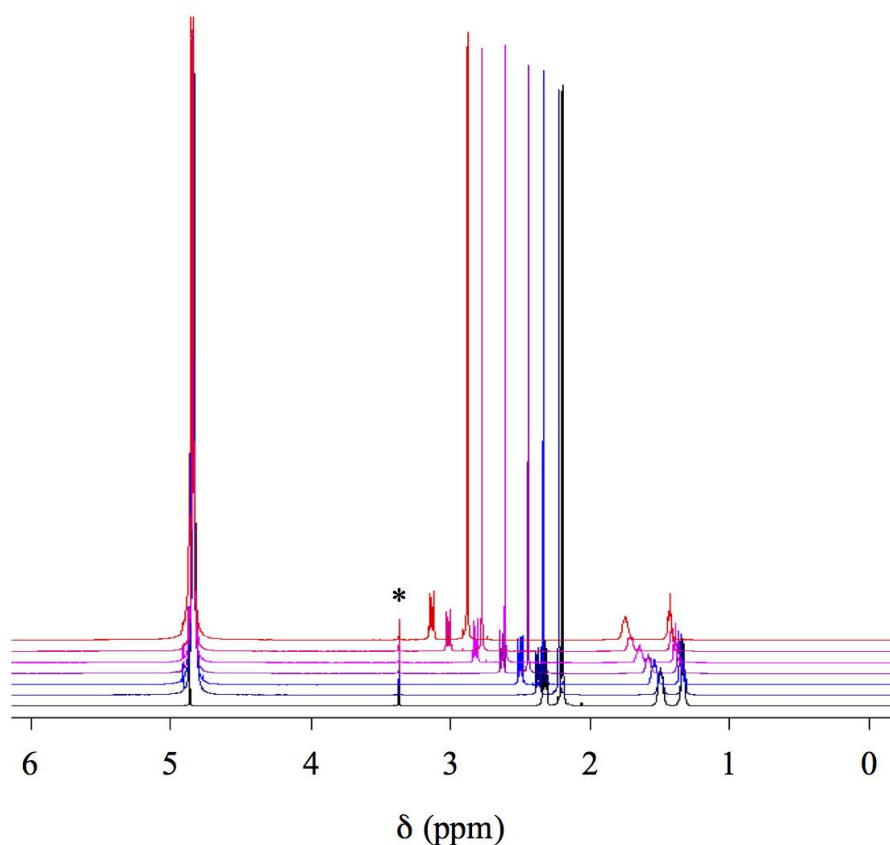


**Figure 11.** <sup>1</sup>H spectra of a TM-Hex solution during CO<sub>2</sub> introduction for 0, 1.5, 10, 20, 40, 70, and 120 min (from the bottom). \* Methanol standard. Solvent: D<sub>2</sub>O. CO<sub>2</sub> flow speed = 500 mL/min for the solution (200 mL). [TM-Hex]<sub>0</sub> = 0.871 M.

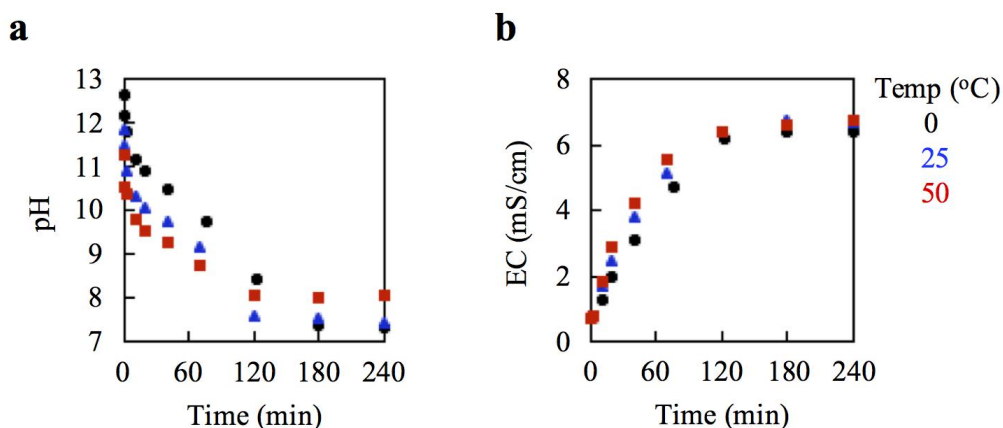


**Figure 12.** The variations in pH (a) and EC (b) of a TM-Hex solution by CO<sub>2</sub> introduction at different temperatures. CO<sub>2</sub> flow speed = 500 mL/min for the solution (200 mL).  
[TM-Hex]<sub>0</sub> = 0.871 M.

The temperature-dependence on the capture of carbonic acid by TM-Hex was also investigated. Figure 12 shows the variations in pH and EC for the CO<sub>2</sub> introduction at 0, 25, and 50°C. Although the gas solubility is in inverse proportion to the temperature in accordance with Henry's law, the pH more rapidly decreased as the temperature increased. This might be attributed to the difference in the initial pH of the diamine solution at the different temperatures. However, this inference was denied based on the fact that the EC increased more rapidly by a temperature increase (Figure 12b). An increase in reactivity of the diamine at high temperature was prior to a decrease in the CO<sub>2</sub> solubility in the water.

The effect of the basicity and structure of the tertiary diamine on the electrolyte formation was explored using TM-Et, TM-Pr, TM-Hex, BDM-Ee, DM-Pip, DABCO, and HMT. Figures 13

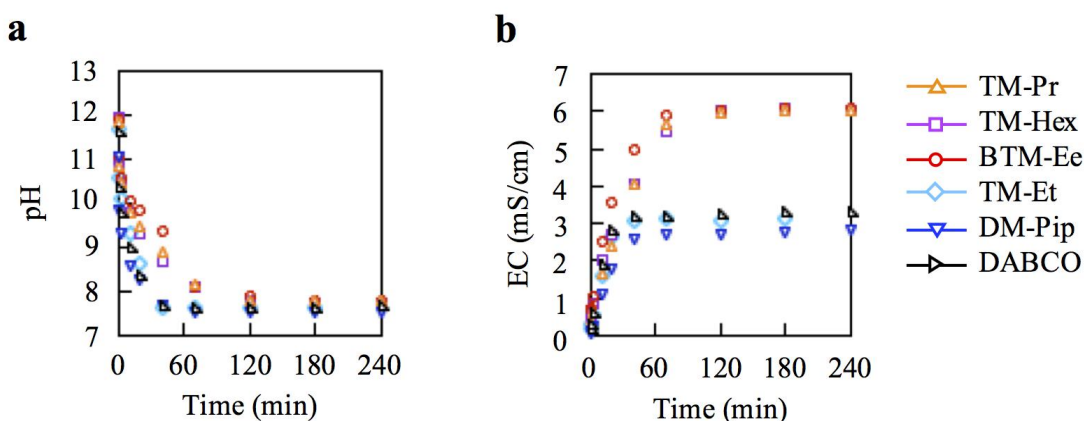
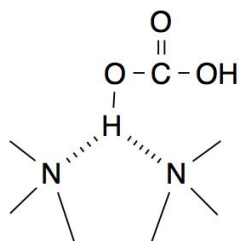


**Figure 13.** The variations in the pH (a) and EC (b) of a solution by CO<sub>2</sub> introduction for different diamines. [diamine]<sub>0</sub> = 1.314 M. CO<sub>2</sub> flow speed = 250 mL/min for the solution (20 mL).

shows variations in the pH and EC of the diamine solutions during the CO<sub>2</sub> introduction. TM-Et, DM-Pip, and DABCO more rapidly decreased the pH than TM-Pr, TM-Hex, and BDM-Ee. However, there was a negligible difference in pH in the steady state. On the other hand, these diamines produced a significant difference in the EC. The former diamine group of TM-Et, DM-Pip, and DABCO produced only half the ECs versus those by the latter diamine group of TM-Pr, TM-Hex, and BDM-Ee. This difference in EC was attributed to their basicity based on the structure. The former group of diamines show a low basicity of pK<sub>a</sub> = 7.67 (TM-Et), 7.99 (DM-Pip), and 8.19 (DABCO) [38], while the latter group of diamines has a high basicity of pK<sub>a</sub> = 9.88 (TM-Pr), 10.07 (TM-Hex), and 9.12 (BDM-Ee). The former diamines have a structure where the N atoms are connected by two methylenes and form an intramolecular five-membered ring via a proton through hydrogen bonding, causing half of the proton capacity for the latter diamines (Scheme 4). In addition, HMT produced no changes in the pH and EC, indicating that it has no ability to capture carbonic acid due to its very low basicity (pK<sub>a</sub> = 5.28) [38].



**Scheme 4. Formation of an intramolecular five-membered ring via a proton through hydrogen bonding for the diamines having the N atoms connected by two methylenes.**

Amines without any nucleophilicity, such as tertiary amines and bulky secondary amines of tetramethylpiperidine can capture CO<sub>2</sub>, however, they often release CO<sub>2</sub> by introduction of inert gases [23-25]. As Ar was introduced into the neutral TM-Hex<sup>2+</sup>2HCO<sub>3</sub><sup>-</sup> solution, the pH increased and became steady at ca. 9 (Figure 14a). When CO<sub>2</sub> was introduced again into the solution, the pH promptly decreased to 7.74. The Ar introduction also produced a change in the EC. The EC was slightly decreased by the Ar introduction, but it was restored by the CO<sub>2</sub> introduction again (Figure 14b). Based on the variations in the pH and EC by the Ar introduction, it was found that the Ar introduction transformed the bicarbonate into the carbonate by releasing some of the bicarbonate anions as CO<sub>2</sub> and vice versa by the second CO<sub>2</sub> introduction (Scheme 5). This reversible bicarbonate-to-carbonate transformation by the alternating introduction of Ar and CO<sub>2</sub> suggests repeatable use of the electrolytes.

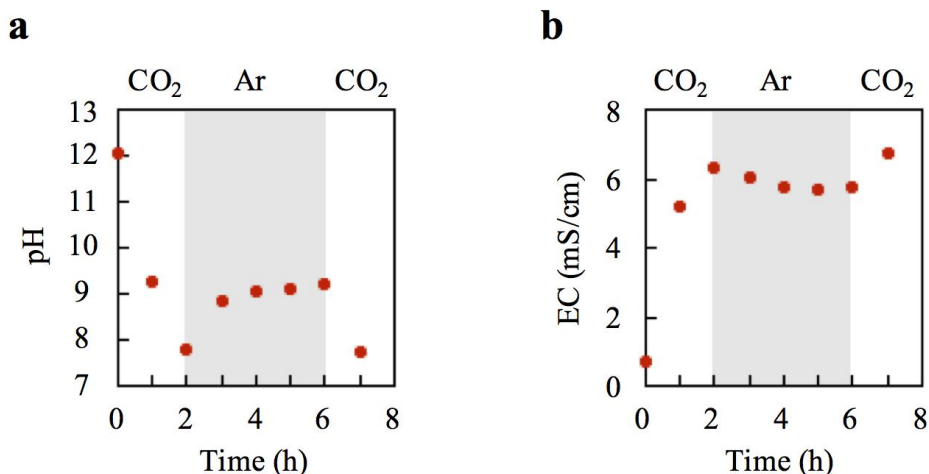
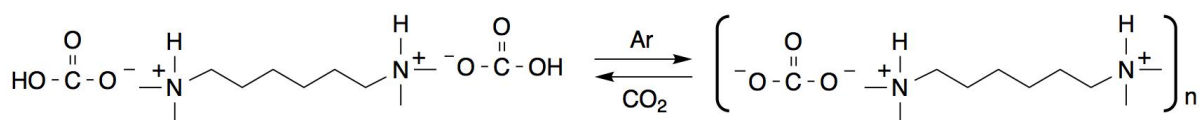


**Figure 14.** The variations in the pH (a) and EC (b) of a TM-Hex solution by CO<sub>2</sub>/Ar alternating introductions. CO<sub>2</sub> flow speed = 250 mL/min and Ar flow speed = 500 mL/min for the solution (20 mL). [TM-Hex]<sub>0</sub> = 1.314 M.



**Scheme 5.** Transformation of the bicarbonate into the carbonate by Ar introduction and vice versa by the second CO<sub>2</sub> introduction.

## 4. Conclusions

The CO<sub>2</sub> capture-induced electrolytes were obtained using the tertiary diamines in an aqueous solution. The electrolytes were formed by the diamines capturing carbonic acid through the formation of the diammonium carbonate, followed by the transformation of the carbonate into the bicarbonate. The EC was dependent only on the protonated diamine concentration. The electrolytes were more effectively produced at a higher temperature despite a decrease in the CO<sub>2</sub> solubility, indicating that the reactivity of the diamine was prior to the CO<sub>2</sub> solubility at high temperature. The basicity and structure of the diamines also affected the EC. The diamines having not less than three methylenes connecting the N atoms effectively produced EC, whereas the diamines with two methylenes between the N atoms generated only half the EC due to the formation of an intramolecular five-membered ring via a proton through hydrogen bonding. The Ar introduction into the bicarbonate solution transformed the bicarbonate into the carbonate, however, the second CO<sub>2</sub> introduction reversed this transformation. This reversible bicarbonate-to-carbonate transformation by the alternating gas

introduction implies the potential of repeatable use of the electrolytes.

## References

- [1] Coumou, D, Rahmstorf, S.A., A decade of weather extremes. *Nature Clim. Change*, 2012, 2, 491-496.
- [2] Flannigan, M, Stocks, B., Turetsky, M., Wotton, M., Impacts of climate change on fire activity and fire management in the circumboreal forest. *Global Change Biol.*, 2009, 15, 549-560.
- [3] Brown, B.E., Coral bleaching: causes and consequences. *Coral Reefs*, 1997, 16, Suppl., S129-S138.
- [4] Hoegh-Guldberg, O., Climate change, coral bleaching and the future of the world's coral reefs. *Mar. Freshwater Res.*, 1999, 50, 839-866.
- [5] Doney, S.C., Ruckelshaus, M., Duffy, J.E., Barry, J.P., Chan, F., English, C.A., Galindo, H.M., Grebmeier, J.M., Hollowed, A.B., Knowlton, N., Polovina, J., Rabalais, N.N., Sydeman, W.J., Talley, L.D., Climate change impacts on marine ecosystems. *Ann. Rev. Mar. Sci.*, 2012, 4, 11-37.
- [6] Burke, M., Hsiang, S.M., Miguel, E., Global non-linear effect of temperature on economic production. *Nature*, 2015, 527, 235-239.
- [7] Marchetti, C., On geoengineering and the CO<sub>2</sub> problem. *Clim. Change*, 1977, 1, 59-68.
- [8] Kazama, S., Teramoto, T., Haraya, K., Carbon dioxide and nitrogen transport properties of bis(phenyl)fluorene-based cardo polymer membranes. *J. Membrane Sci.*, 2002, 207, 91-104.
- [9] Vonshak, A., Guy, R., Photoadaptation, photoinhibition and the blue-green alga, *Spirulina platensis* grown outdoors. *Plant: Cell Environ.*, 1992, 15, 613-616.
- [10] Laws, W.A., Berning, J.L., A study of the energetics and economics of microalgal mass culture with the marine chlorophyte *Tetraselmis suecica*: Implications for use of power plant stack gases. *Biotechnol. Bioeng.*, 1991, 37, 936-947.
- [11] Könneke, M., Schubert, D.M., Brown, P.C., Hügler, M., Standfest, S., Schwander, T., von Borzyskowski, L.S., Erb, T.J., Stahl, D.A., Berg, I.A., Ammonia-oxidizing archaea use the most energy efficient aerobic pathway for CO<sub>2</sub> fixation. Proceedings of the National Academy of Sciences of the United State of America. *PNAS*, 2014, 111, 8239-8244.

- [12] Samuelov, N.S., Lamed, R., Lowe, S., Zeikus, J.G., Influence of CO<sub>2</sub>-HCO<sub>3</sub><sup>-</sup> levels and pH on growth, succinate production, and enzyme activities of anaerobiospirillum succiniciproducens. *Appl. Environ. Microbiol.*, 1991, 57, 3013-3019.
- [13] Kikuchi, S., Yoshida, S., Sugawara, Y., Yamada, W., Cheng, H., Fukui, K., Sekine, K., Iwakura, I., Ikeno, T., Yamada, T., Silver-catalyzed carbon dioxide incorporation and rearrangement on propargylic derivatives. *Bull. Chem. Soc. Jpn.*, 2011, 84, 698-717.
- [14] Inoue, S., Tsuruta, T., Furukawa, J., Preparation of optically active poly(propylene oxide) by asymmetric induction. *Makromol. Chem.*, 1962, 53, 215-218.
- [15] Koinuma, H., Hirai, H., Copolymerization of carbon dioxide and oxetane. *Makromol. Chem.*, 1977, 178, 241-246.
- [16] Soga, K., Hosoda, S., Tazuke, Y., Ikeda, S., Copolymerization of carbon dioxide and ethyl vinyl ether. *J. Polym. Sci., Polym. Lett. Ed.*, 1975, 13, 265-268.
- [17] Tsuda, T., Maruta, K., Kitaike, Y., Nickel(0)-catalyzed alternating copolymerization of carbon dioxide with diynes to poly(2-pyrones). *J. Am. Chem. Soc.*, 1992, 114, 1498-1499.
- [18] Kihara, N., Endo, T., Catalytic activity of various salts in the reaction of 2,3-epoxypropyl phenyl ether and carbon dioxide under atmospheric pressure. *J. Org. Chem.*, 1993, 58, 6198-6202.
- [19] Aresta, M., Dibenedetto, A., Carone, M., Colonna, T., Fragale, C., Production of biodiesel from macroalgae by supercritical CO<sub>2</sub> extraction and thermochemical liquefaction. *Environ. Chem. Lett.*, 2005, 3, 136-139.
- [20] Marrone, C., Poletto, M., Reverchon, E., Stassi, A., Almond oil extraction by supercritical CO<sub>2</sub>: experiments and modelling. *Chem. Eng. Sci.*, 1998, 53, 3711-3718.
- [21] van der Kraan, M., Fernandez Cid, M.V., Woerlee, G.F., Veugelers, W.J.T., Witkamp, G.J., Dyeing of natural and synthetic textiles in supercritical carbon dioxide with disperse reactive dyes. *J. Supercrit. Fluids*, 2007, 40, 470-476.
- [22] Sicardi, S., Manna, L., Banchero, M., Diffusion of disperse dyes in PET films during impregnation with a supercritical fluid. *J. Supercrit. Fluids*, 2000, 17, 187-194.
- [23] Yan, Q., Zhou, R., Fu, C., Zhang, H., Yin, Y., Yuan, J., CO<sub>2</sub>-responsive polymeric vesicles that breathe. *Angew. Chem. Int. Ed.* 2011, 50, 4923-4927.
- [24] Pinaud, J., Kowal, E., Cunningham, M., Jessop, P., 2-(Diethyl)aminoethyl methacrylate as a CO<sub>2</sub>-switchable comonomer for the preparation of readily coagulated and redispersed polymer latexes. *ACS Macro Lett.*, 2012, 1, 1103-1107.
- [25] Yoshida, E., CO<sub>2</sub>-responsive behavior of polymer giant vesicles supporting hindered amine. *Colloid Polym. Sci.*, 2019, 297, 661-666.

- [26] MacDowell, N., Florin, N., Buchard, A., Hallett, J., Galindo, A., Jackson, G., Adjiman, C.S., Williams, C.K., Shah, N., Fennell, P., An overview of CO<sub>2</sub> capture technologies. *Energy Environ. Sci.*, 2010, 3, 1645-1669.
- [27] Lashaki, M.J., Khiavi, S., Sayari, A., Stability of amine-functionalized CO<sub>2</sub> adsorbents: a multifaced puzzle. *Chem. Soc. Rev.*, 2019, 48, 3320-3405.
- [28] Ding, M., Flaig, R.W., Jiang, H., Yaghi, O.M., Carbon capture and conversion using metal–organic frameworks and MOF-based materials. *Chem. Soc. Rev.*, 2019, 48, 2783-2828.
- [29] Zhang, X., Zhang, X., Dong, H., Zhao, Z., Zhang, S., Huang, Y., Carbon capture with ionic liquids: overview and progress. *Energy Environ. Sci.*, 2012, 5, 6668-6681.
- [30] Bae, T., Hudson, M.R., Mason, J.A., Queen, W.L., Dutton, J.J., Sumida, K., Micklash, K.J., Kaye, S.S., Brown, C.M., Long, J.R., Evaluation of cation-exchanged zeolite adsorbents for post-combustion carbon dioxide capture. *Energy Environ. Sci.*, 2013, 6, 128-138.
- [31] Ichikawa, S., Seki, T., Tada, M., Iwasawa, Y., Ikariya, T., Amorphous nano-structured silicas for high-performance carbon dioxide confinement. *J. Mater. Chem.*, 2010, 20, 3163-3165.
- [32] Paura, E.N.C., da Cunha, W.F., Roncaratti, L.F., Martins, J.B.L., e Silva, G.M., Gargano, R., CO<sub>2</sub> adsorption on single-walled boron nitride nanotubes containing vacancy defects. *RSC Adv.*, 2015, 5, 27412-27420.
- [33] Hartono, A., Rennemo, R., Awais, M., Vevelstad, S.J., Brakstad, O.G., Kim, I., Knuutila, H.K., Characterization of 2-piperidineethanol and 1-(2-hydroxyethyl)pyrrolidine as strong bicarbonate forming solvents for CO<sub>2</sub> capture. *Int. J. Greenhouse Gas Control*, 2017, 63, 260-271.
- [34] Xiao, M., Cui, D., Zou, L., Yang, Q., Gao, H., Liang, Z., Experimental and modeling studies of bicarbonate forming amines for CO<sub>2</sub> capture by NMR spectroscopy and VLE. *Sep. Purif. Technol.*, 2020, 234, 116097.
- [35] Wei, Z., Lin, Z., Niu, H., He, H., Ji, Y., Simultaneous desulfurization and denitrification by microwave reactor with ammonium bicarbonate and zeolite. *J. Hazard. Mater.*, 2009, 162, 837-841.
- [36] Aasanuma, N., Harada, M., Nogami, M., Suzuki, K., Kikuchi, T., Tomiyasu, H., Ikeda, Y., Anodic dissolution of UO<sub>2</sub> pellet containing simulated fission products in ammonium carbonate solution. *J. Nuclear Sci. Technol.*, 2006, 43, 255-262.

- [37] Voskian, S., Hatton, T.A., Faradaic electro-swing reactive adsorption for CO<sub>2</sub> capture. *Energy Environ. Sci.*, 2019, 12, 3530-3547.
- [38] Calculated using Advanced Chemistry Development (ACD/Labs) Software V11.02 (1994-2020 ACD/Labs). Basicity in SciFinder.